

# Stellar Population of the Irregular Galaxy IC 10<sup>1</sup>

N. A. Tikhonov and O. A. Galazutdinova

*Special Astrophysical Observatory, Russian Academy of Sciences, N. Arkhyz, KChR, 369167, Russia*

Received October 10, 2008

## ABSTRACT

Based on our observations with the 6-m BTA telescope at the Special Astrophysical Observatory, the Russian Academy of Sciences, and archival Hubble Space Telescope images, we have performed stellar photometry for several regions of the irregular galaxy IC 10, a member of the Local Group. Distance moduli with a median value of  $(m - M) = 24.47$ ,  $D = 780 \pm 40$  kpc, have been obtained by the TRGB method for several regions of IC 10. We have revealed 57 star clusters with various masses and ages within the fields used. Comparison of the Hertzsprung - Russell diagrams for star clusters in IC 10 with theoretical isochrones has shown that this galaxy has an enhanced metallicity, which probably explains the high ratio of the numbers of carbon and nitrogen Wolf-Rayet stars (WC/WN). The size of the galaxy's thick disk along its minor axis is 10.5 and a more extended halo is observed outside this disk.

## Introduction

The irregular galaxy IC 10 is a member of the Local Group and is at a relatively close distance. However, it still remains a mysterious object in both morphology and physical parameters. Since the galaxy is located in the Milky Way zone ( $b = -3.^\circ 3$ ), its light undergoes strong extinction in gas-dust clouds of our Galaxy. This creates difficulties in studying IC 10, because some of its characteristics are known to within the extinction.

IC 10 ranks fifth in luminosity in the Local Group, being less luminous than large spiral galaxies (M31, MW, M33) and a bright irregular galaxy — the Large Magellanic Cloud. The integrated spectrophotometry of IC 10 by (Hunter & Gallagher 1985) revealed intense star

---

<sup>1</sup>Based on observations made with the NASA/ESA Hubble Space Telescope, obtained from the Data Archive at the Space Telescope Science Institute, which is operated by the Association of Universities for Research in Astronomy, Inc., under NASA contract NAS5-26555. These observations are associated with proposals 6404, 7912, 9633, 9676, 9683 and 10242

formation processes in the galaxy. This is also confirmed by the images of IC 10 showing that the central galactic regions contain a large number of bright young stars ((de Vaucouleurs 1965; Karachentsev & Tikhonov 1993). The existence of bright and extended H II regions in the galaxy is also indicative of star formation activity (Hodge and Lee 1990).

One of the peculiarities of IC 10 is a high space density of young Wolf-Rayet stars, exceeding that in ordinary irregular galaxies ((Massey et al. 1992; Massey & Armandroff 1995; Royer et al. 2001; Massey & Holmes 2002; Crowther et al. 2003)). In addition, an unusually large ratio of the numbers of carbon and nitrogen (WC/WN) Wolf-Rayet stars is observed, which is in conflict with the low ( $Z = 0.3Z_{\odot}$ ) metallicity of the interstellar medium in IC 10 found by (Lequeux et al. 1979) and (Garnett 1990).

The presence of star formation over large areas of the galaxy, the high surface brightness, and the bluish color (after correction for the galactic reddening) gave (Richer 2001) reason to believe IC 10 to be a blue compact galaxy. This classification emphasizes that IC 10 is at a short stage of a starburst affecting significant volumes of the galaxy.

Observations of the neutral hydrogen ( $H I$ ) in IC 10 were first performed by (Roberts 1962), who discovered a hydrogen cloud around the galaxy. The structure of this cloud with an angular resolution of  $2'$  and its sizes were determined by (Shostak 1974), who found the cloud to be approximately elliptical in shape and to rotate slowly. (Huchtmeier 1979) and (Cohen 1979) ascertained that the sizes of the hydrogen cloud reach one degree, which is hardly comparable to the galaxy's apparent sizes of  $5.9' \times 6.8''$ . A detailed map of the H I distribution in IC 10 with an angular resolution of  $5'$  was obtained by (Wilcots & Miller 1998), who found that the structurally complex hydrogen cloud of IC 10 has shells and holes produced by stellar winds from bright WR and O stars. (Thurow & Wilcots 2005) studied in detail the kinematics of the ionized gas in IC 10 and determined the gas velocity dispersion in various morphological structures: shells, regions around Wolf-Rayet stars, and interstellar voids. Thus, the hydrogen observations also confirm the activity of star formation processes in IC 10.

## OBSERVATIONAL DATA AND STELLAR PHOTOMETRY

Figure 1 presents a DSS2 image of IC 10 with the labeled fields of various telescopes and detectors that we used. To study the stellar structure of this galaxy, we used both ground-based observations with the 6-m BTA telescope and the 1-m Zeiss telescope at the Special Astrophysical Observatory and archival data from the Hubble Space Telescope (HST) with the WFPC2, ACS/WFC, and STIS cameras. Since the images from the 1-m Zeiss telescope and several fields from the 6-m BTA telescope were used for the most part to search for variable objects in IC 10, they are not marked in Fig. 1. General information about the observations is given in Table 1. For several areas of the galaxy, the images with different detectors overlap: WFPC2 and ACS/WFC, ACS/WFC and 6-m BTA, STIS, and

---

<sup>2</sup>NASA/IPAC Extragalactic Database

ACS/WFC. This allows us to compare the photometric results and, if necessary, to identify objects with a variable luminosity. The WFPC2 and ACS/WFC images were used to study the spatial distribution of stars with various ages in IC 10 and to reveal star clusters, while the observations with the STIS camera and the 6-m BTA telescope (fields ST2, ST3, F5, and F7) were used to determine the boundary of the stellar subsystem – the galactic thick disk.

The photometric reduction of both ground-based and space images was performed with the DAOPHOT II package (Stetson 1994) in MIDAS. For the HST ACS/WFC images, we used the DOLPHOT package (Dolphin 2000a,b) for stellar photometry, which allowed us to compare the photometric results of the two programs and to check the accuracy of our results. We subjected the images from the ground-based BTA telescope to a standard primary reduction and transformed instrumental magnitudes to Kron-Cousins magnitudes based on the equations derived during the photometry of standard stars from the list by (Landolt 1992).

Figure 2 presents the results of our stellar photometry in the form of Hertzsprung-Russell (color- magnitude or CM) diagrams. Since the CM diagrams for some fields are almost identical, we presented only the most characteristic results. Whereas Fig. 2a presents the diagram for the entire ACS1 field, Fig. 2b presents the results only for the part of the ACS2 field that we used to determine the distance. The diagrams for the full ACS2 and ACS3 fields differ little from the diagram for the ACS1 field. There is an analogous similarity for fields F5 and F7 of the 6-m BTA telescope and for fields ST1, ST2, and ST3 of the HST STIS camera.

Branches of young stars (blue and red supergiants), a densely populated and wide branch of red giants, and a branch of AGB stars are seen on all diagrams for the central regions of IC 10, especially on the deep ACS/WFC ones. In general, if the strong reddening of all stars is disregarded, then the CM diagram for IC 10 does not differ in any way from the CM diagrams for irregular starburst galaxies: NGC 1569, NGC 4214, Ho II, and others.

## EXTINCTION IN IC 10

Since, as has already been said, an accurate determination of the extinction is a key to measuring the galaxy’s parameters, let us consider the measurement of this quantity in more detail. A great variety of methods for estimating the extinction toward IC 10 can be found in publications. As a rule, the values obtained were used to determine the distance to the galaxy.

Since gas-dust clouds are clearly seen in the images of IC 10, it is highly likely that there is light absorption and scattering in the galaxy itself, which must vary over the body of the galaxy quite nonuniformly. This means that, apart from the extinction in gas-dust clouds of our Galaxy (external component), there must be extinction in the galaxy IC 10 itself (internal component). It is the combined action of these components that creates the complex pattern of extinction that, as will be shown below, is observed in IC 10.

Since the stars owe their origin to the existence of gas-dust clouds, it can be assumed that the extinction in IC 10 will roughly correspond to the apparent distribution of young stars that have not yet receded far from their parent gas-dust complexes. Figure 3 shows the apparent distribution of blue and red supergiants in the central regions of IC 10. Large nonuniformities in the distribution of young stars can be seen in the figure. This confirms the well-known fact that the stars originate in individual complexes and points to the possible places of clumpy inhomogeneities leading to extinction fluctuations. However, this method cannot reveal any gas-dust clouds on the periphery of IC 10 outside star-forming regions or those in our Galaxy in the path of light propagation from IC 10.

Our study of the stellar subsystems in irregular galaxies showed that thick stellar disks with a monotonic number density distribution of their constituent stars, red giants, exist in all galaxies (Tikhonov 2005, 2006). Thus, the spatial distribution of red giants in IC 10 must be fairly smooth, without large number density fluctuations, because judging by its morphology, IC 10 belongs to irregular galaxies. This fact can be used to reveal the fluctuations of light-absorbing matter, provided that it is located between the disk of IC 10 and the observer. However, if we construct the apparent distribution of red giants located on a particular CM diagram (Fig. 2), then the fluctuations in the number density of stars will have a very low contrast against the general background due to the effect of extinction in gas-dust clouds, since the passage of light through gas-dust clouds leads to its reddening and attenuation and displaces the star on the CM diagram but does not bring out the star far outside the red giant branch. This means that almost all of the red giants, except the faintest ones, will remain in the list and will be involved in constructing the apparent distribution of stars. To see the distribution of precisely those stars that underwent an excessive reddening compared to the mean value for the entire galaxy, we should choose the stars located at the „red” edge of the red giant branch and construct their apparent distribution. In choosing such stars on the CM diagram, we used the following parameters:  $23 < I < 25$  and  $(I + 4 \times (V - I) - 33) > 1$ . The luminosity was constrained to remove faint stars with low photometric accuracy and AGB stars with a spatial number density distribution differing in shape from that of red giants and the expression in parentheses separates out the necessary part of the red giant branch. The distribution of excessively reddened stars constructed in this way is presented in Fig. 4. As expected, an increase in the concentration of such stars (i.e., the places of highest reddening) near the regions of young stars can be seen, but this dependence is rather weak. A more interesting result is the appearance of zones of strong extinction outside the concentration regions of young stars. These dark zones correspond either to gas-dust clouds on the periphery of IC 10 or to clouds in our Galaxy (which is unlikely). In Fig. 4, we clearly see a filamentary-clumpy pattern of lightabsorbing dark clouds even within the small (in size) ACS/WFC field.

The deviation of the extinction from its mean value for various regions of IC 10 can be estimated using again red giants. Constructing the luminosity function of red giants for various regions of the galaxy and determining the beginning of the red giant branch (TRGB jump) on the diagrams, we obtain the pattern of change in the position of the TRGB jump from region to region due to the differences in extinction. It should be noted that if the matter absorbing the transmitted light is located within the thick disk of IC 10 whose stars we use, then the TRGB jump in the luminosity function will be smeared, because there will

be stars undergoing different extinctions in our sample.

Choosing small (in size) regions in the places of high and low concentration of reddened stars, i.e., in the zones of maximum and minimum extinction, we constructed the luminosity functions for them and found that the difference in extinction in the I band reached  $I = 1^m3$  in them. This leads to an additional reddening reaching  $E(V - I) = 0^m9$ . In many cases, the TRGB jump was smeared, which can be explained by the location of the red giants and lightabsorbing matter in the same spatial volume of the galaxy. The maximum extinction in IC 10 is observed in a small dark nebula at the southeastern edge of the galaxy. The main-sequence stars are successively shifted there to  $(V - I) = 2^m4$ , corresponding to an extinction of  $6^m$  in the V band.

These results show the entire complexity of extinction measurements, irrespective of the method used. Therefore, it is not surprising that the distance measurements for IC 10 gave a spread in values from 0.25 to 3.0 Mpc. Summarizing the results, we can say that the extinction toward IC 10 estimated from observations depends noticeably on the place of its measurement and we can talk only about its local value. Moreover, the significant extinction fluctuations over the body of the galaxy cast doubt on the results of distance measurements by some methods, since objects located in regions with both high and low extinctions are involved in the measurement process. This is primarily true for the method of Cepheids, when a small sample of stars is used, and for the method of brightest stars.

Comparison of the map of the H I distribution ((Wilcots & Miller 1998)) with our map of excessively reddened red giants (Fig. 4) shows only their partial similarity. The filaments of excessive reddening in Fig. 4 coincide in position with the H I filaments, but the region with highly reddened stars at the edge of Fig. 4 does not correspond to any isolines of the H I distribution in IC 10. At the same time, we see in the composite color image of IC 10<sup>3</sup> that this region is only part of a more extended dark ring structure around the starburst region. The global inhomogeneities of light-absorbing matter can be seen in the infrared DSS2 images, but no small local inhomogeneities comparable in size to those in Fig. 4 are seen in them.

## DISTANCE DETERMINATION

The long-established fact that IC 10 belongs to the Local Group ((de Vaucouleurs 1965)) is beyond question, but the precise distance to this galaxy still remains a variable quantity. Table 2 gives the distances obtained by different methods and using different extinctions. We see from the results presented in Table 2 that the authors often overestimate the accuracy of their measurements. The long-used method of Cepheids could give a reliable distance to IC 10, but only if a large number of Cepheids is used in order to average the individual extinctions. The results of distance measurements where the extinction is calculated on the basis of one or two Cepheids ((Saha et al. 1996; Wilson et al. 1996)) may be considered to be

---

<sup>3</sup><http://www.lowell.edu/users/massey/lgsurvey.html>

nothing more than approximate estimates, bearing in mind the large extinction fluctuations. Even when ten Cepheids are used ((Sakai et al. 1999), a scatter of points (up to  $2^m$ ) is observed on the period-luminosity diagram and, in the long run, only two or three Cepheids determine the distance modulus being obtained. To achieve agreement between their result and the result based on the TRGB method, the authors have to arbitrarily introduce an additional extinction at the galactic center. An extreme example of inappropriateness of the method of Cepheids can be seen in the publications by (Wilson 1995) and (Wilson et al. 1996), where the distance estimate for IC 10 changed from 240 to 820 kpc.

Using red supergiants ((Karachentsev & Tikhonov 1993; Borissova et al. 2000; Ovcharov & Nedialkov 2005)) to determine the distance to IC 10 seems doubtful, because the luminosity of the brightest red supergiants depends strongly on their metallicity and individual extinction, not to mention the calibration accuracy of the method itself. The as yet inadequately developed method of carbon stars used by (Demers et al. 2004) also has critical remarks on the correction of extinction, the luminosity of the objects used, and the effect of metallicity.

Using the luminosity function of red giants and determining the cutoff point of the giant branch (the TRGB method by (Lee et al. 1993)) gives a reliable distance, but only under one condition: if the extinction is known for these stars. The extinction fluctuation in the galaxy’s central regions causes the position of ITRGB to change from  $21^m8$  to  $23^m0$  from region to region. This makes the results by (Tikhonov 1999) and (Sakai et al. 1999) improper, since the TRGB method was used by these authors for large areas of the galaxy.

We attempted to circumvent these causes of inappropriateness of the TRGB method and, for this purpose, chose several star-forming regions in IC 10 with a large number of blue supergiants. Based on the change in the position of the reddened blue supergiant branches on the diagram relative to their normal position, which was determined by the use of isochrones with  $Z = 0.008$  and  $Z = 0.02$ , we calculated the extinctions for specific regions that we used for the subsequent work with red giants. Such a method was applied by (Massey & Armandroff 1995) for the entire area of IC 10. Our distinction was that we used images not from ground-based telescopes but from the HST. This made it possible to construct a CM diagram for any region of the galaxy, even dense star complexes unresolvable into stars by ground-based telescopes. In addition, during each measurement, we used a very small region of the galaxy to reduce the extinction fluctuations and determined the shift of the blue supergiant branch relative to its normal position not on the basis of visual estimates but by fitting isochrones from (Bertelli et al. 1994) with different metallicities into the CM diagrams, while calculating not only the extinction but also the metallicity and age of the star complex.

During our measurements, it emerged that not all regions of young stars could be used to determine the distance by this method. Four of the 20 chosen regions had an unblurred TRGB boundary, indicating that, in most cases, the red giants and gas-dust matter are located in the same volume of the galaxy. For each region, we constructed the luminosity function of red giants and found the cutoff point of the red giant branch (TRGB jump) and its color index. Correcting the magnitudes for extinction and using equations from (Lee et al. 1993), we found the distance moduli for the galaxy for various regions containing clusters (Table 3) in regions containing clusters:

N20 :  $E(V - I) = 1.50$ ,  $(m - M) = 24.48$ ,  $[Fe/H] = -1.28$ ,  $D = 786 \pm 50$  kpc;

N36 :  $E(V - I) = 1.21$ ,  $(m - M) = 24.75$ ,  $[Fe/H] = -1.40$ ,  $D = 890 \pm 60$  kpc;

N48 :  $E(V - I) = 1.04$ ,  $(m - M) = 24.65$ ,  $[Fe/H] = -1.22$ ,  $D = 854 \pm 50$  kpc;

N54 :  $E(V - I) = 1.05$ ,  $(m - M) = 24.45$ ,  $[Fe/H] = -0.93$ ,  $D = 780 \pm 50$  kpc.

Since the extinction gradient undesirable for the method of distance determination is observed over the entire apparent body of the galaxy, we also used WFPC2 images obtained away from the galactic center (Fig. 1) to determine the distance. A densely populated branch of giants and a weak branch of blue stars can be seen on the CM diagram for this field (Fig. 2f). The images of this region were used by (Sanna et al. 2007) to determine the distance. Applying the TRGB method, we first checked the region for extinction fluctuations and, for our measurements, chose only part of the image at ( $0 < X < 600$  pixels), where the number density of excessively reddened stars was almost constant over the field, indicative of a constant extinction. Since the region of measurements is far from the galactic center and since no star-forming regions are observed nearby, while the distribution of faint blue stars is uniform over the field, we believe that this branch of blue stars consists of old stars rather than main-sequence ones, as was assumed by (Sanna et al. 2007). The same old blue stars are seen in large quantities in the central regions of M31 and M32, where no star formation processes are observed. In the evolutionary sequence, these blue stars are low-mass core-helium-burning stars with ages of several Gyr. The old age of IC 10 indicates that such stars can exist in this galaxy, since we found stars in the blue part of the horizontal branch for several old globular clusters in IC 10, which can be observed only in old star clusters. The color index of the branch of these blue stars can be found using isochrones from (Bertelli et al. 1994). For the luminosity constraints  $1.5 < M_I < 0$  and metallicity  $Z = 0.008$  and  $Z = 0.004$ , we found the color index of such stars with ages of 7–9 Gyr to be  $(V - I) = -0.33$ . Taking this value, determining the position of the reddened branch of such stars at  $(V - I) = 0.68$ , and using relations from (Karachentsev & Tikhonov 1993), we found the extinction in this direction:  $A_I = 1.43$ . For the red giants of the region, we determined the TRGB jump in the luminosity function and the color index of the red giant branch:  $I_{TRGB} = 21.87$ ,  $(V - I)_{-3.5} = 2.47$ , and  $(V - I)_{TRGB} = 2.8$ . Using equations from (Lee et al. 1993), we determined the metallicity of red giants and the distance to IC 10 in region S3 (Fig. 1):  $E(V - I) = 1.01$ ,  $[Fe/H] = -1.28$ ,  $(m - M) = 24.44$ ,  $D = 770 \pm 50$  kpc.

The drawback of the result obtained is the small number of blue stars used to determine the extinction. Therefore, we attempted to apply this approach for a field area in the ACS/WFC image closer to the galactic center. We chose small areas in the ACS/WFC images where there were virtually no extinction gradient and where no star-forming regions were observed. Only one area of field A2 located at the greatest distance from the galactic center satisfies all these conditions:  $2500 < X < 3500$  pixels and  $Y > 2800$  pixels. For this area, we found that the faint blue stars lie at  $(V - I) = 0.83$ . Since the normal color index of these stars is  $(V - I) = -0.33$ , the reddening is  $E(V - I) = 1.16$  and the extinction is  $A_I = 1.64$ . The TRGB jump in the luminosity function of red giants lies at  $I_{TRGB} = 22.03$ , while the color of the red giant branch is  $(V - I)_{-3.5} = 2.65$  and  $(V - I)_{TRGB} = 2.95$ . Using equations from (Lee et al. 1993), we found for this area:  $E(V - I) = 1.16$ ,  $[Fe/H] = -1.19$ ,  $(m - M) = 24.42$ ,  $D = 765 \pm 50$  kpc.

Thus, we obtained distances for six fields of the galaxy. Since the median averaging of the results gives a more accurate value than the simple average, applying it for our six values yields the final results:  $[Fe/H] = -1.22$ ,  $(m - M) = 24.47$ ,  $D = 780 \pm 40$  kpc. The derived distance to IC 10 indicates that the galaxy is located at the same distance as the massive galaxies M31 and is away from it only in the plane of the sky. Comparison of the metallicity of red giants in IC 10 with the metallicity of giants in other irregular or low-mass spiral galaxies shows that IC 10 is not a metal-poor galaxy but more likely has an enhanced metallicity.

## STAR CLUSTERS

For many years, it has been unknown which types of star clusters are present in IC 10 and whether they exist there at all. (Karachentsev & Tikhonov 1993) pointed out seven candidates for star clusters in IC 10 and (Georgiev et al. 1996) provided photometric data on them. Based on HST ACS/WFC images, we checked these possible clusters and found that four of them are actually star clusters, while three probable clusters are outside the available HST images. Based on HST WFPC2 images, (Hunter 2001) pointed out 13 star clusters and associations with various ages and masses. A check of the list by (Hunter 2001) based on deep ACS/WFC images showed that the two clusters identified by this author (4–6 and 4–7) are single stars, while clusters 4–1 and 4–2 are most likely parts of the same extended star complex. At the same time, the old globular cluster, N56 in our list, clearly seen in WFPC2 was not included in the list. We found no other papers on the search for star clusters in IC 10.

Using the Large Magellanic Cloud (LMC) as an example, we see that irregular galaxies can contain both young star clusters with various masses and old clusters ((Baade 1966)). Since the physical parameters of IC 10 are close to those of the LMC, we also expected to find a similar variety of star clusters in IC 10, a galaxy with a central starburst and an extended subsystem in the form of a thick disk of old stars ((Tikhonov 1999; Magrini 2003; Demers et al. 2004)).

Based on a visual examination of the images for IC 10, primarily fields A1 and A2 (Fig. 1), we identified more than 50 clusters with various masses and ages. To avoid the errors in identifying poor clusters, we took into account the diffuse halo around the cluster, better seen in the V images, that is produced by faint unresolvable main-sequence stars in young clusters or by faint red giants and horizontal-branch stars in old clusters. Naturally, the completeness of our sample decreases when identifying poor and old clusters; not the visual method but a computer algorithm should be used for their identification. The results of our search for clusters are presented in Table 3, which gives their coordinates, the sizes of their visually seen part, and morphology. The true sizes of the star complexes can exceed significantly those given in Table 3, because their periphery is lost among the numerous background stars.

The images that we used cover almost the entire central part of IC 10 with star-forming regions near which young clusters are located, but several more young clusters can be found

in the western part of the galaxy that is not covered by the HST images. As regards the old globular clusters, the discovery of several clusters is also possible here, because much of the galactic periphery remains unstudied. The example of the WFPC2 image (field S2 in Fig. 1) in which an old globular cluster was found on the galactic periphery is revealing.

All of the star clusters found can be separated into young, old, and intermediate-age ones. In turn, the young clusters can be separated into star complexes, bright globular clusters, and open or compact poor clusters. The old clusters can be separated into bright globular and faint clusters, while the intermediate-age clusters have a low brightness and contain faint main-sequence stars and faint red supergiants. Within the HST ACS/WFC images, we found: 8 young complexes, 10 young open clusters, 12 young compact clusters, 5 young globular clusters, 5 intermediate-age clusters, 5 old open clusters, and 12 old globular clusters. In this list, one old globular cluster (N1) was found in the WFPC2 image (field S2) and one old globular cluster (N49) was taken from (Karachentsev & Tikhonov 1993). Thus, IC 10 has star clusters of the same types as those in the LMC, which confirms a morphological similarity of these galaxies, except the slightly lower mass of IC 10.

When separating the clusters by their age into young and old ones, we used stellar photometry and CM diagrams for the clusters found. Some of the clusters have a high star density and the stellar photometry of such clusters is possible only on their periphery. In these cases, the CM diagram for a cluster can contain a significant number of background stars from the disk of IC 10 that are projected onto the cluster region. The resulting mixture of stars with various ages creates an uncertainty in the separation of the clusters into young and old ones. To make the separation procedure more objective, we selected a strip in the galactic image with the center in the cluster under study and plotted the number density distribution of old or young stars along this strip. If the cluster is young, then the number density of young stars will peak on the plot at the point corresponding to the position of the cluster center. A similar picture will be observed when the distribution of red giants or horizontal-branch stars is constructed for an old cluster. The ACS/WFC images of several young and old clusters found are shown in Fig. 5. One of the old globular clusters (N10) is very elongated in shape. This can be explained either by an optical superposition of two clusters, which is unlikely, or by the result of a gravitational interaction between a cluster and the galaxy. Note that similar elongated globular clusters are present in the LMC, thereby confirming a morphological similarity of the two galaxies.

Having the tables of stellar photometry for IC 10 at our disposal, we constructed CM diagrams for several young complexes and compared them with isochrones from (Bertelli et al. 1994). Since the sizes of all complexes do not exceed several arcsec, the extinction may be assumed to be approximately the same for all stars of the same complex. This is confirmed by the small width of the blue supergiant branch in each complex. On the derived diagrams, we see that the color index of the blue supergiant branch changes from complex to complex, which directly indicates that the extinction is different for different regions of the galaxy. In their measurements, (Lequeux et al. 1979) and (Garnett 1990) obtained a low metallicity ( $Z = 0.3Z_{\odot}$ ) for H II regions in IC 10. Therefore, it can be assumed that the isochrones with  $Z = 0.008$  will describe well our CM diagrams. However, comparison showed (Fig. 6) that the isochrones with  $Z = 0.02$ , i.e., with a solar metallicity, provide the best fit. Since this comparison was made for several star complexes containing red supergiants, it can be

argued that IC 10 is not a metal-poor galaxy, as has been assumed up until now. Having identified bright stars with large color indices (among which there can also be red dwarfs of our Galaxy), we constructed their apparent distribution over the body of IC 10. The concentrations of such stars coincident with star-forming regions or compact clusters can be seen in the derived distribution. This proves that these stars belong to bright red supergiants but not to foreground dwarfs of our Galaxy. Thus, it should be recognized that the brightest supergiants with ages of 15-30 Myr in many young clusters of IC 10 have a solar metallicity.

The high metallicity of stars in IC 10 that we found may remove the contradiction between the excessively large ratio of the numbers of carbon and nitrogen (WC/WN) Wolf-Rayet stars and the low metallicity of the galaxy assumed so far. Because of the large number of clusters found, their detailed study is a matter of a separate paper that we are planning to present in the immediate future.

## THE SIZES OF THE GALACTIC THICK DISK AND HALO

Whereas IC 10 has an irregular shape in the visual spectral range, a disk with a regular shape that consists mostly of red stars and has an axial ratio  $a/b = 1.38$  is seen on the 2MASS infrared ( $K_s$ -band) images. Clearly, we see only the central part of the disk, where AGB stars with ages from 100 to 800 Myr make the largest contribution to its emission. To see the distribution of old RGB stars that constitute the thick disk of IC 10, it is necessary to identify these stars on the CM diagram and to construct their apparent distribution over the body of the galaxy. Unfortunately, the insufficient angular sizes of the available images and the extinction fluctuations over the body of the galaxy lead to a distortion of the actual distribution of stars, but even the available data indicate that the stellar subsystems of IC 10 are similar in structure to those of irregular galaxies. Since the thick-disk sizes for most irregular galaxies determine the maximum sizes of the galaxies, it seems interesting to identify the thick disk in IC 10. The existence of this stellar subsystem can be seen from the exponential decrease in the number density of red giants toward the galactic edge in all of the images we used. The size of the thick disk in IC 10 was first determined by (Tikhonov 1999) based on images from the 6-m BTA telescope. The derived disk diameter of 18 was minimal, because the thick-disk boundary was not reached. Subsequently, additional images from the 6-m BTA telescope were used and the thick-disk boundary along the galaxy's minor axis was found to pass at a galactocentric distance of 10.5 and a more extended halo stretches further out ((Tikhonov 2002; Drozdovsky et al. 2003)). A jump in the number density of stars and a change in the density gradient are observed (Fig. 7) at the thick-disk boundary (fields F5 and F7 in Fig. 1), corresponding to the passage from the thick disk to the halo. If the outer disk has the same axial ratio as the inner one, then the thick disk is  $29' \times 21'$  in size. The thick disk that we identified is indicated in Fig. 1 in the form of an ellipse. The number density distributions of stars in fields ST2 and ST3 give an additional confirmation of the validity of the thick-disk boundary. In the former case, a simple decrease in the number density of stars is observed; in the latter case, a change in the density gradient is seen, although these data are not very reliable due to the small number of stars available in these fields.

The halo whose far boundary has not yet been determined is even larger in size than the

thick disk. Based on the distribution of red giants, (Demers et al. 2004) found the maximum sizes of IC 10 to be  $32'$ . In their figure, the distribution has the shape of a horseshoe, which is the result of an inhomogeneous extinction in IC 10 and a low photometric limit of the images used. It is beyond doubt that the halo of IC 10 has larger sizes than those of the galaxy given by (Demers et al. 2004).

(Huchtmeier 1979) and (Cohen 1979) found the hydrogen disk of IC 10 to be more than one degree in size. Does the stellar halo extend to the same distance? Solving this question can also give an answer to the question about the origin of the hydrogen cloud around the galaxy. Does the cloud arise (at least partially) from the mass loss by stars or it has an external origin, forming when a remote gas falls to the galaxy? For many of the galaxies we investigated, the sizes of the hydrogen cloud have never exceeded those of the stellar disks or halo, including, for example, those for such an irregular galaxy as NGC 2915 with apparent sizes of  $1.'0 \times 1.'9$ , while the hydrogen disk is at least  $20'$  with a distinct spiral structure. When the stellar subsystems of IC 10 are studied, its fairly close neighbor, the giant spiral galaxy M31, should be kept in mind. The gravitational interaction between the two galaxies can change significantly the morphology of IC 10 even if this interaction took place in the distant past.

## RESULTS AND CONCLUSIONS

For several regions of IC 10, we performed deep stellar photometry based on which we constructed Hertzsprung-Russel diagrams for stars of both central regions and periphery of the galaxy. The derived CM diagrams for IC 10 do not differ in any way from those for irregular starburst galaxies. Distance moduli with a median value of  $(m - M) = 24.47$ ,  $D = 780 \pm 40$  kpc, were obtained for six galactic fields by the TRGB method. Our study of the distribution of red giants revealed extinction inhomogeneities reaching  $\delta I = 1^m3$  or  $E(V - I) = 0^m9$  within the investigated galactic fields. Such inhomogeneities create difficulties in determining the distance to the galaxy and measuring its physical parameters. A visual examination of the images and our stellar photometry revealed 57 star clusters in the galaxy with various ages and masses. Comparison of the CM diagrams for clusters with theoretical isochrones allowed us to determine the ages and metallicities of cluster stars. The metallicities of young supergiants in IC 10 were found to be nearly solar. This means that IC 10 has an enhanced metallicity, which probably also explains the high ratio of the numbers of carbon and nitrogen Wolf-Rayet stars (WC/WN). We determined the size of the thick disk in IC 10 along its minor axis by measuring the gradient in the number density of red giants:  $B = 10.'5$ . The halo, which also consists of old stars, extends to an even greater distance. It may well be that the size of the halo will coincide to that of the hydrogen cloud around IC 10, i.e., will have a diameter of at least one degree.

Our results close some gaps in the investigation of IC 10 and provide a basis for further studies. In particular, the star clusters of IC 10 should be studied in more detail to compare their parameters with those of clusters in other irregular galaxies. The questions about the sizes of the stellar halo in IC 10 and the structure of its outer periphery still also remain unanswered, since the possible interaction of IC 10 with M31 could change the morphology

of the thick disk and halo in IC 10, particularly their outer parts. The high metallicity of young stars in IC 10 that we obtained requires accurate spectroscopic observations of young supergiants to confirm these results, which may well be performed in the immediate future.

## REFERENCES

- Baade, W., *Evolution of Stars and Galaxies* (Harvard Univ., Cambridge, Mass. 1963; Mir, Moscow, 1966)
- Bertelli, G., Bressan, A., Chiosi, C. et al. 1994, *A&A*, 106, 275
- Borissova, J., Georgiev, L., Rosado, M. et al. 2000, *A&A*, 363, 130
- Bottinelli, L., Gougenheim, L., Paturel, G. & de Vaucouleurs, G. 1984, *A&AS*, 56, 381
- Cardelli, J. A., Clayton, G. C. & Mathis J. S. 1989, *ApJ*, 345, 245
- Cohen, R. J. 1979, *MNRAS*, 187, 839
- Crowther, P. A., Drisse, L., Abbott, J. B. et al. 2003, *A&A*, 404, 483
- Demers, S., Battinelli, P. & Letarte, B. 2004, *A&A*, 424, 125
- Dolphin, A. E. 2000a, *PASP*, 112, 1383
- Dolphin, A. E. 2000b, *PASP*112, 1397
- Drozdovsky, I., Tikhonov, N., Schulte-Ladweg, R. & Aparicio, A., 2003, *IAUS* 221, 57
- Garnett, D. R. 1990, *ApJ*, 363, 142
- Georgiev, Ts. B., Tikhonov, N. A. & Karachentsev, I. D. 1996, *Astron. Astrophys. Trans.* 11, 47
- Huchtmeier, W. K. 1979, *A&A*, 75, 170
- Hunter, D. A. 2001, *A&A*, 559, 225
- Hunter, D. A. & Gallagher, J. S. III, 1985, *A&AS*, 58, 533
- Jacoby, J. & Lesser, M. 1981, *AJ*, 86, 185
- Karachentsev, I. D. & Tikhonov, N. A. 1993, *A&AS*, 100, 227
- Landolt, A. U. 1992 *AJ*, 104, 340
- Lee, M. G., Freedman, W. L. & Madore, B. F. 1993, *ApJ*, 417, 553
- Lequeux, J., Peimbert, M., Rayo, J. F. et al. 1979, *A&A*, 80, 155
- Magrini, L., Corradi, R. L. M., Greimel, R. et al. 2003, *A&A*, 407, 51
- Massey, P. & Armandroff, T. E. 1995, *AJ*, 109, 2470

- Massey, P. & Holmes, S. 2002, ApJ, 580, L35
- Massey, P., Armandroff, T. E. , & Conti P. S. 1992 AJ, 103, 1159
- Ovcharov, E. & Nedialkov, P. 2005, Aerospace Res. Bulgaria, 20, 85
- Richer, M. G., Bullejos, A., Borissova, J. et al. 2001 A&A, 370, 34
- Roberts M. S. 1962, AJ, 67, 431
- Royer, P., Smartt, S. J., Manfroid, J., & Vreux, J. M. 2001, A&A, 366, L1
- Saha, A., Hoessel, J. G., Krist J. & Danielson, G. E. 1996, AJ, 111, 197
- Sakai, S., Madore, B. F. & Freedman, W. L. 1999, ApJ, 511, 671
- Sandage, A. & Tammann, G. 1994, ApJ, 194, 559
- Sanna, N., Bono, G., Monelli, M. et al. 2007, Mem. Soc. Astron. It., 79, 3
- Shostak, G. S. 1974 A&A, 31, 97
- Stetson, P. B. 1994 PASP, 106, 250
- Thurrow, J. C. & Wilcots E. M. 2005 AJ, 129, 745
- Tikhonov, N. A., in The Stellar Content of Local Group Galaxies, Proc. of the 192 IAU Symp., Ed. by P. A. Whitelock and R. D. Cannon (ASP, San Francisco, 1999), p. 244.
- Tikhonov, N. A. 2002, Doctoral Phys.-Math. Dissertation, St.-Peterb. Gos. Univ., St. Petersburg
- Tikhonov, N. A. 2005, Astron. Rep., 49, 501
- Tikhonov, N. A. 2006, Astron. Rep., 50, 517
- Vacca, W. D., Sheehy, C. D. & Graham J. R. 2007, ApJ, 662, 272
- de Vaucouleurs, G. 1978, ApJ, 224, 710
- de Vaucouleurs, G. & Ables, H. 1965, PASP, 77, 272
- Wilcots, E. M. & Miller, B. W. 1998, AJ, 116, 2363
- Wilson, C. D. , The Local Group: Comparative and Global Properties, Ed. by A. Layden, R. C. Smith, and J. Storm, ESO Workshop Proc. No. 51 (ESO Garching, 1995), p. 15.
- Wilson, C. D., Welch, D. L., Reid, I. N. et al. 1996, AJ, 111, 1106

Table 1: Observational data.

Date	Telescope	Field	Filter	Exposure	Proposal ID
June 1997	HST WFPC2	S1	F814W	$1400 \times 10$	6406
July 1998	6-m BTA	F5	I	600	
July 1998	6-m BTA	F5	R	600	
June 1999	HST WFPC2	S1	F555W	$1400 \times 10$	6406
June 1999	HST STIS	ST1	(V)*	$1200 \times 2$	7912
June 1999	HST STIS	ST1	(I)*	$1200 \times 2$	7912
Jan. 1999	6-m BTA	F1	I	600	
Jan. 1999	6-m BTA	F1	R	600	
Oct. 2000	6-m BTA	F7	I	$300 \times 3$	
Oct. 2000	6-m BTA	F7	R	$300 \times 3$	
Oct. 2002	HST STIS	ST2	(V)*	$480 \times 2$	9633
Oct. 2002	HST STIS	ST2	(I)*	$\Sigma = 800$	9633
Oct. 2002	HST STIS	ST3	(V)*	$480 \times 2$	9633
Oct. 2002	HST STIS	ST3	(I)*	$\Sigma = 800$	9633
Oct. 2002	HST WFPC2	S2	F606W	$500 \times 2$	9676
Oct. 2002	HST ACS/WFC	A1	F606W	2160	9683
Oct. 2002	HST ACS/WFC	A1	F814W	2160	9683
Oct. 2002	HST ACS/WFC	A2	F606W	$1080 \times 2$	9683
Oct. 2002	HST ACS/WFC	A2	F814W	$1080 \times 2$	9683
Jan. 2005	HST WFPC2	S3	F555W	$500 \times 12$	10242
Jan. 2005	HST WFPC2	S3	F814W	$500 \times 12$	10242
Jan. 2005	HST ACS/WFC	A3	F555W	$2480 \times 8$	10242
Jan. 2005	HST ACS/WFC	A3	F814W	$2380 \times 4$	10242

Note. (V)\* and (I)\* are broadband filters that we reduced to the international V and I bands.

Table 2: Results of distance measurements for IC 10

$D$ , Mpc	$\sigma$	$E(B - V)$	Method	Authors
1.5	–	–	H II rings	Roberts (1962)
1.25	–	0.87	H II rings	de Vaucouleurs & Ables (1965)
3.0	0.3	0.78	H II rings	Sandage & Tammann (1974)
2.0	0.4	0.40	H II rings	de Vaucouleurs (1978)
1.8	0.5	0.78	Planetary nebulae	Jacoby & Lesser (1981)
2.0	–	0.40	Tully-Fisher	Bottinelli et al. (1984)
1.04	0.09	0.87	Brightest stars	Karachentsev & Tikhonov (1993)
0.24	–	1.55	Cepheids	Wilson (1995)
0.95	0.09	0.80	Wolf-Rayet stars	Massey & Armandroff (1995)
0.82	0.08	0.80	Cepheids	Wilson et al. (1996)
0.83	0.11	0.94	Cepheids	Saha et al. (1996)
0.58	0.05	0.98	Tip of the red giant branch	Tikhonov (1999)
0.66	0.07	1.16	Cepheids	Sakai et al. (1999)
0.50	0.05	0.85	Tip of the red giant branch	Sakai et al. (1999)
0.59	0.05	1.05	Brightest stars	Borissova et al. (2000)
0.74	0.04	0.79	Carbon stars	Demers et al. (2004)
0.72	0.11	1.25	Brightest stars	Ovcharov & Nedialkov (2005)
0.78	0.03	0.95	Tip of the red giant branch	Vacca et al. (2007)
0.89	0.04	0.60	Tip of the red giant branch	Sanna et al. (2007)
0.78	0.05	0.80	Tip of the red giant branch	This paper (2009)

Table 3: Star clusters in IC 10

No.	<i>RA</i>	<i>DEC</i>	Size, arcsec	Cluster morphology
01	00 19 53.98	+59 13 25.7	3.0	Old globular, bright
02	00 19 57.84	+59 19 53.3	1.5	Intermediate age, open
03	00 19 59.25	+59 19 35.7	0.8	Young, compact, bright
04	00 20 00.16	+59 19 58.6	2.8	Old globular, faint
05	00 20 02.05	+59 19 45.5	1.5	Young globular, poor
06	00 20 02.05	+59 20 04.7	0.6	Young, compact, bright
07	00 20 02.22	+59 19 07.7	1.5	Old globular, faint
08	00 20 03.19	+59 18 50.5	1.9	Old open, faint
09	00 20 04.34	+59 18 34.9	2.0	Old open, poor
10	00 20 05.68	+59 18 26.5	3.2	Old globular, very elongated
11	00 20 06.57	+59 19 22.5	1.7	Young open, poor
12	00 20 06.68	+59 19 09.0	1.2	Old open, poor
13	00 20 07.53	+59 19 16.3	1.2	Old globular, faint
14	00 20 07.58	+59 19 26.7	1.4	Young, compact, bright
15	00 20 09.64	+59 17 19.2	2.3	Young globular, bright
16	00 20 10.45	+59 18 22.2	0.8	Young, compact, poor
17	00 20 10.47	+59 21 07.3	1.5	Old, open, poor
18	00 20 11.50	+59 18 50.9	1.6	Young, open, bright
19	00 20 12.37	+59 19 16.8	1.6	Young globular, bright
20	00 20 12.40	+59 17 27.7	2.6	Young globular, bright
21	00 20 13.92	+59 21 14.7	1.0	Old, compact, poor
22	00 20 15.42	+59 19 49.8	0.6	Intermediate age, compact
23	00 20 17.23	+59 17 01.6	3.4	Old globular, bright
24	00 20 17.24	+59 17 45.3	2.8	Young globular, bright
25	00 20 17.37	+59 16 56.1	2.7	Young open, poor
26	00 20 17.71	+59 19 17.5	1.3	Young open, poor
27	00 20 17.86	+59 17 46.3	0.9	Young, compact, bright
28	00 20 17.89	+59 17 01.9	4.1	Young, open, bright
29	00 20 18.03	+59 19 50.5	3.7	Old globular, bright
30	00 20 18.45	+59 17 58.4	1.0	Young, compact, bright
31	00 20 18.42	+59 18 23.4	1.4	Old globular, faint
32	00 20 18.63	+59 18 55.3	5.5	Young complex with bright stars
33	00 20 18.94	+59 18 08.9	1.0	Young, compact, bright
34	00 20 19.19	+59 17 30.3	1.6	Old globular, faint
35	00 20 20.07	+59 18 20.9	1.4	Young, open, poor
36	00 20 20.37	+59 18 37.7	1.4	Core of wide young complex
37	00 20 20.96	+59 17 13.1	2.0	Young open, poor
38	00 20 21.02	+59 18 59.5	1.1	Intermediate age, compact, poor
39	00 20 21.71	+59 18 22.4	1.0	Young, compact, poor
40	00 20 21.79	+59 17 41.0	0.6	Young, very compact, bright
41	00 20 22.43	+59 17 15.5	9.6	Young complex with bright stars
42	00 20 23.09	+59 16 52.9	0.5	Intermediate age, compact, poor
43	00 20 23.74	+59 17 33.1	1.2	Young open, poor
44	00 20 24.21	+59 19 10.1	2.8	Intermediate age, open, rich
45	00 20 24.51	+59 18 18.1	2.1	Young open, poor
46	00 20 24.69	+59 18 11.8	1.0	Young, compact, bright
47	00 20 25.04	+59 17 39.2	2.8	Young, open, rich
48	00 20 27.36	+59 21 14.6	2.5	Old globular, bright
50	00 20 26.76	+59 17 02.5	1.0	Young, compact, poor
51	00 20 26.67	+59 19 48.0	1.3	Old globular, faint
52	00 20 27.48	+59 17 23.4	2.6	Young complex with bright stars
53	00 20 27.48	+59 17 07.7	0.4	Young, very compact, poor
54	00 20 27.80	+59 17 38.4	3.8	Young complex with bright stars
55	00 20 29.15	+59 16 57.8	7.2	Young complex with bright stars
56	00 20 29.57	+59 18 07.5	1.2	Old globular, faint
57	00 20 32.18	+59 17 12.1	1.8	Core of wide young complex

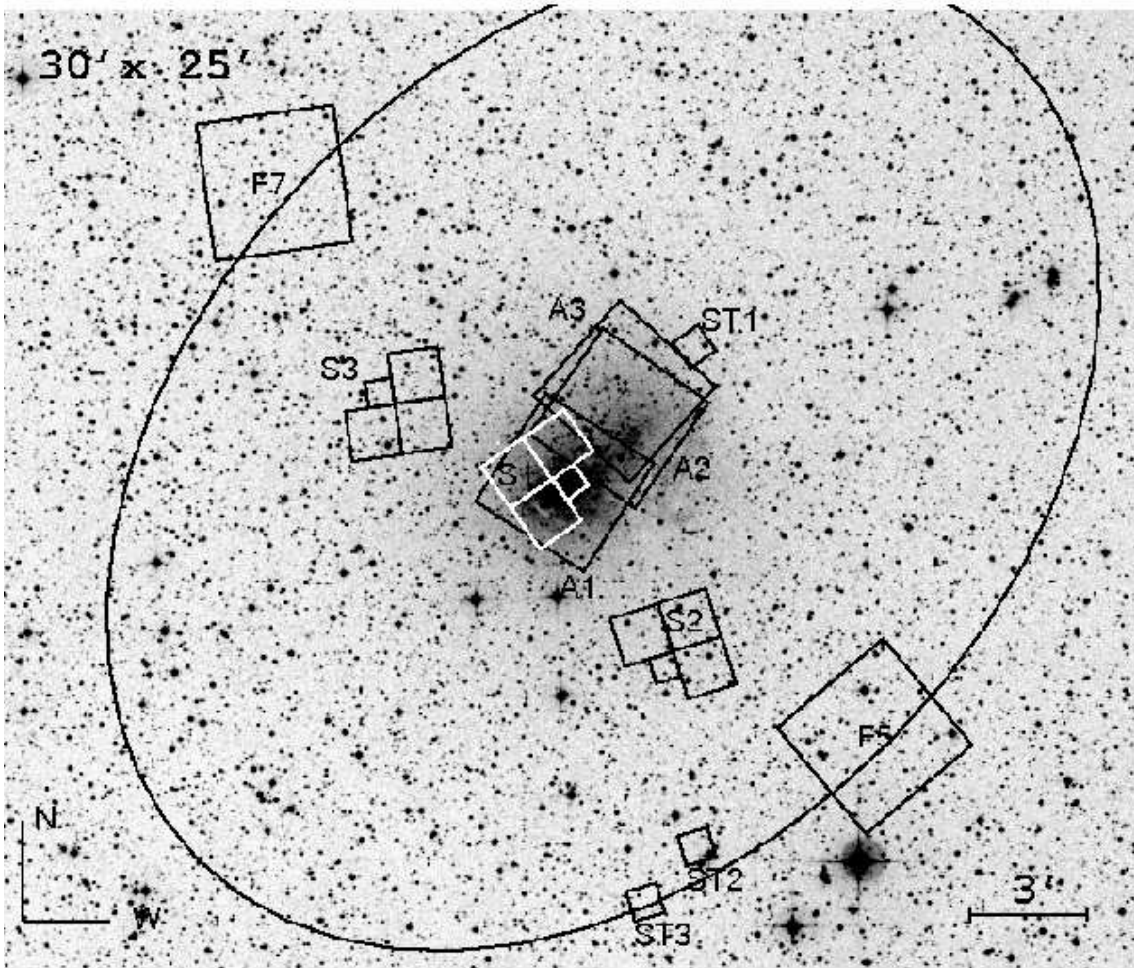


Fig. 1.— DSS2 image of IC 10. The fields that we used in studying the galaxy’s stellar composition are labeled: F5 and F7 for the 6-m BTA telescope; ST1, ST2, ST3 for the STIS camera; S1, S2, S3 for the WFPC2 camera; A1, A2, A3 for the HST ACS/WFC camera. The ellipse marks the boundary between the thick disk and the more extended halo.

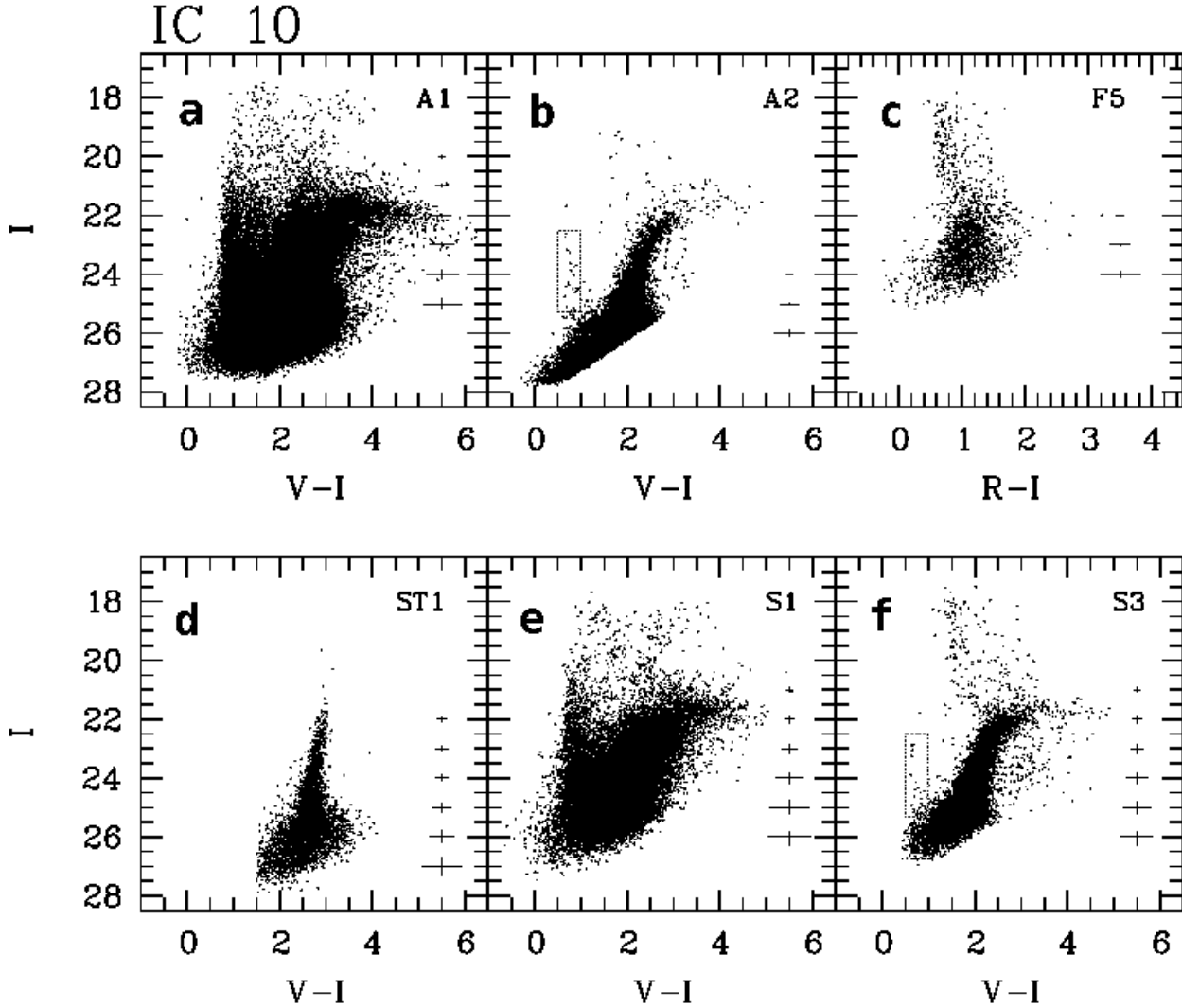


Fig. 2.— Hertzsprung-Russell diagrams for various regions of IC 10: (a) and (e) star-forming regions (ACS1 and WFPC2); (b) a field far from the galactic center (ACS2); (c) thick-disk periphery (F5); (d) and (f) fields in the thick disk (ST1 and WFPC2). On the CM diagrams for the ACS2 and WFPC2 fields, the branches of old blue stars of these fields are marked.

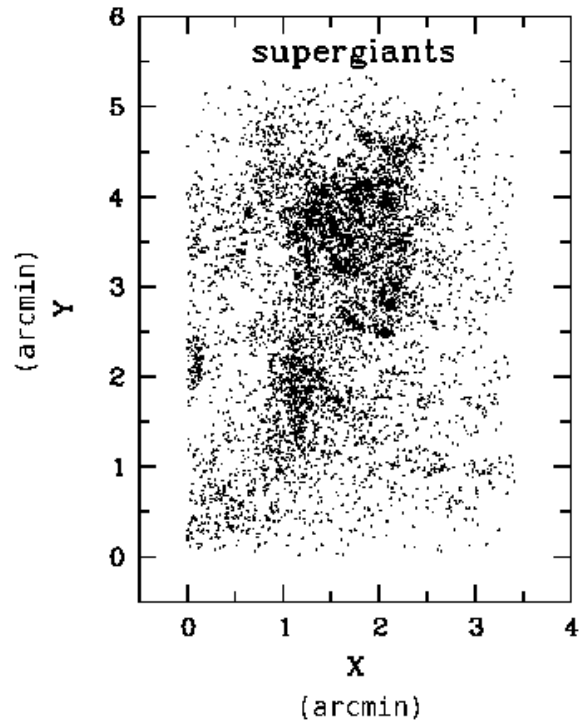


Fig. 3.— Apparent distribution of young supergiants in the galaxy’s central regions (fields A1 and A2). The concentration zones of young stars point to the places of a possible excessive reddening of stars due when light passes through gas-dust clouds of IC 10.

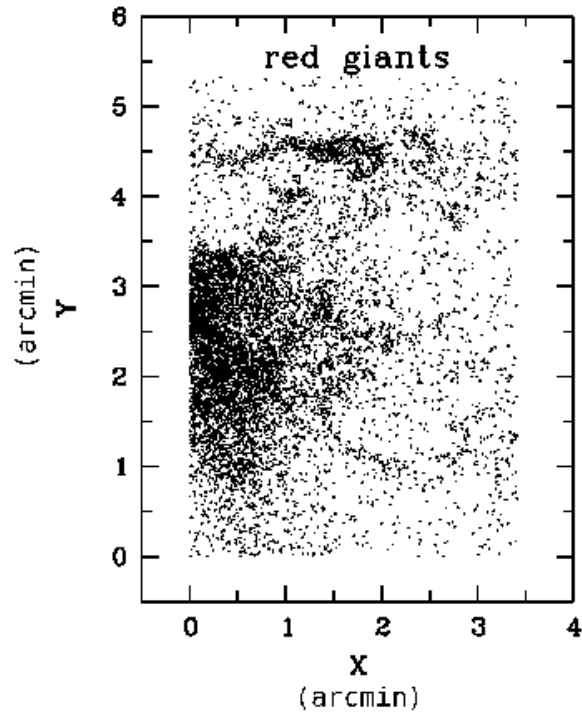


Fig. 4.— Apparent distribution of excessively reddened red giants. The field boundaries correspond to those in Fig. 3. The narrow filaments with a concentration of reddened stars correspond to the positions of H I filaments. The wide region of concentration of reddened stars seen in the left part of the figure does not correspond to any significant H I clouds, but corresponds to the dark regions seen on the composite color image of IC 10.

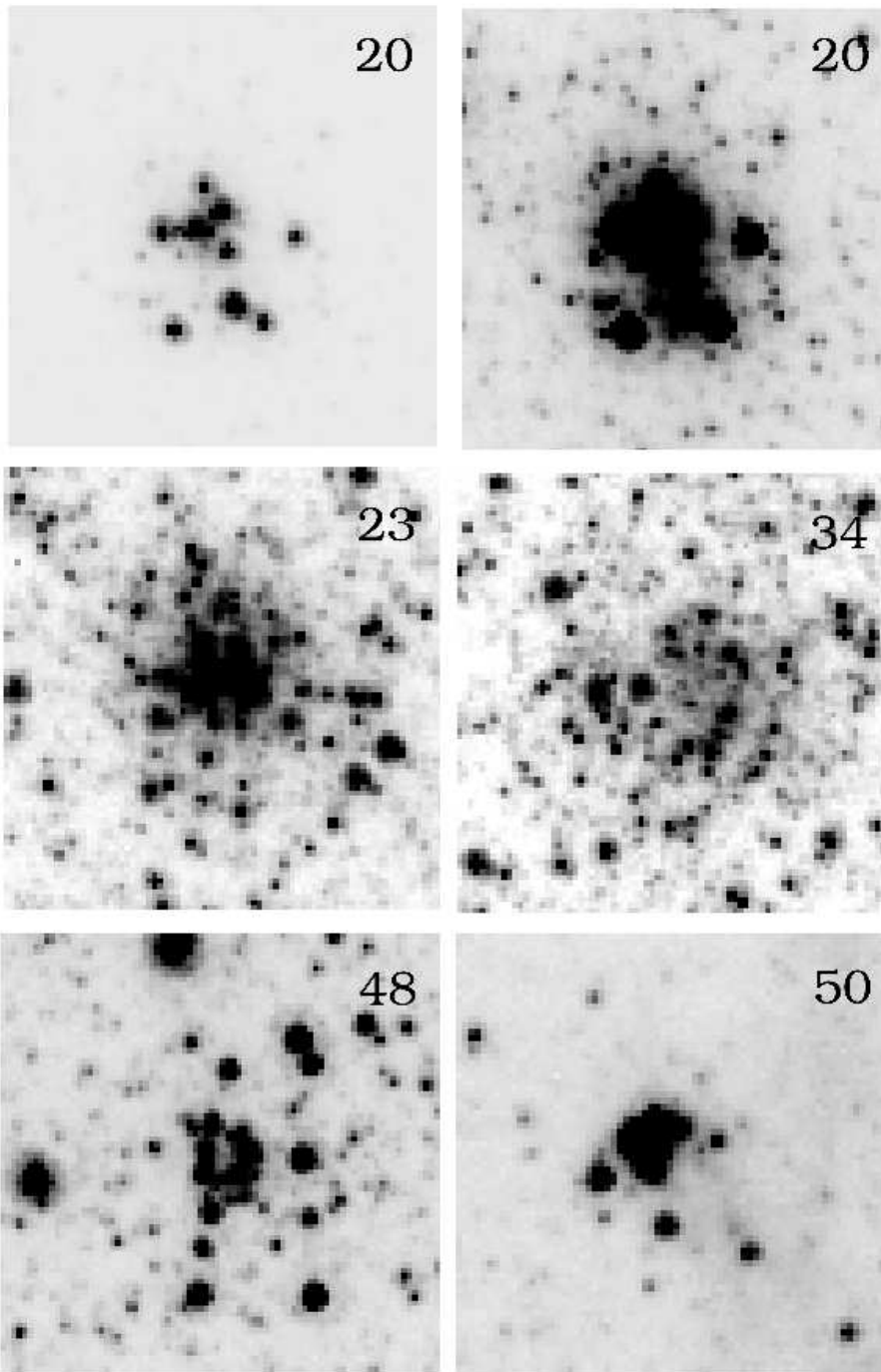


Fig. 5.— ACS/WFC images of several clusters in IC 10: two images of N20 with different reproduction conditions – a young globular cluster with red supergiants, N23 – an old globular cluster, N34 – a young open cluster, N48 – the core of a wide star complex, N50 – a compact young cluster.

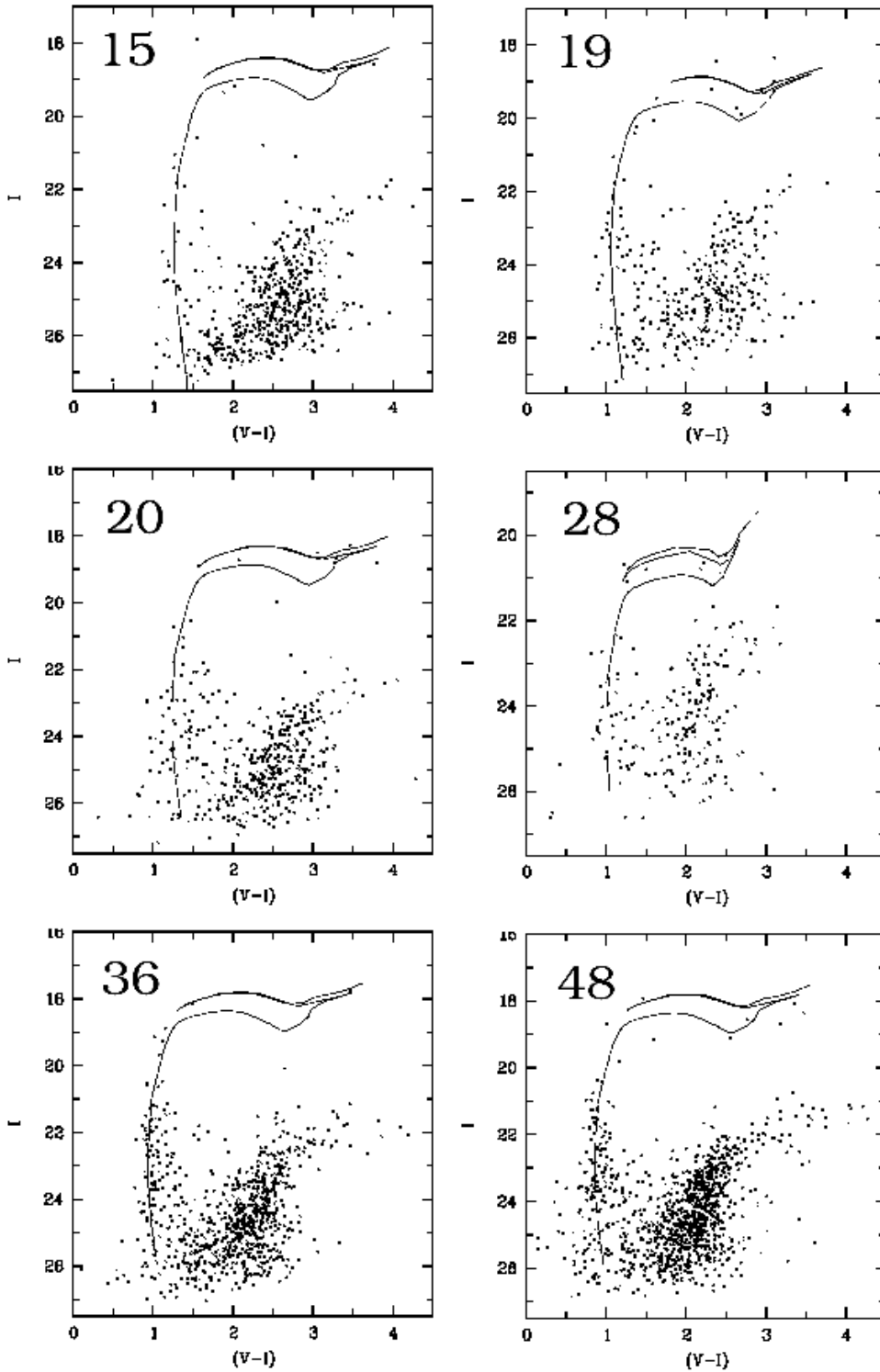


Fig. 6.— CM diagrams for the clusters N15, N19, N20, N28, N36, and N48 with fitted  $t = 13$  Myr isochrones and metallicity  $Z = 0.02$ , except N28, where the isochrone with metallicity  $Z = 0.008$  was fitted. We see that bright red supergiants with a high metallicity equal to the solar one are present in most of the presented clusters. On the diagrams, we see that the blue supergiant branches have different color indices, indicating that the extinction varies from cluster to cluster.

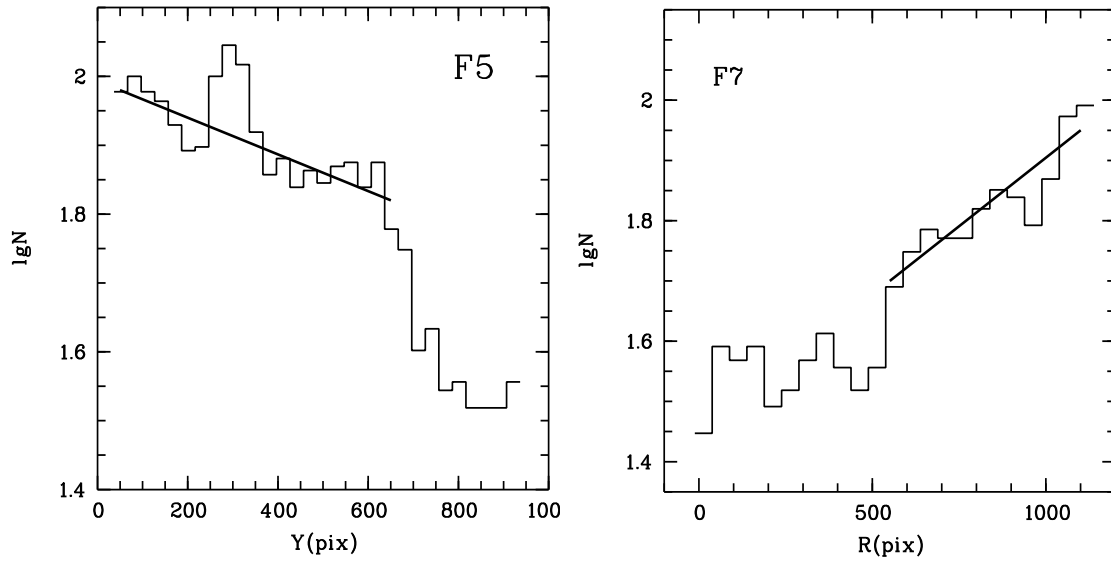


Fig. 7.— Change of the gradient in the number density of red giants at the boundary of the thick disk and halo in fields F5 and F7. Outside the thick disk at  $B = 10.5$ , the gradient in the number density of red giants decreases sharply, but the halo still extends to a considerable distance from the galactic center.